

Statistical multistep reactions: Application

H. Kalka, M. Torjman, and D. Seeliger

Sektion Physik, Technische Universität Dresden, German Democratic Republic

(Received 8 June 1988)

A model for statistical multistep direct and multistep compound reactions is presented. It predicts (double-differential) neutron and proton spectra including equilibrium, preequilibrium, direct (collective and noncollective) as well as multiple particle emission processes. Calculations for nucleon-induced reactions have been performed for about 30 nuclei at incident energies between 5 and 26 MeV without any parameter fit.

I. INTRODUCTION

Over the years, nuclear reaction mechanisms have been investigated within the theoretical concepts of statistical multistep compound (SMC) (Refs. 1-7) and statistical multistep direct (SMD) processes.^{2,3,8-10} Until now, a lot of experimental data have been compared either within a pure SMC model^{2,11-13} or within a pure SMD approach.^{8,14} But in nucleon-nucleus reactions at bombarding energies between 5 and 30 MeV (which are of interest for nuclear engineering) both SMC and SMD processes are important. For this purpose, a SMD-SMC model including direct collective excitations was proposed in Ref. 15. In subsequent papers^{16,17} this model was improved and derived from a Green's function formalism³ and random matrix physics.^{1,18} In this respect we try to overcome the gap between refined theories (which are too complicated for application) and simple-to-handle models for nuclear data evaluation.

In this paper we limit ourselves to the basic ideas of the SMD-SMC model. A brief foundation of this model and comparisons with other approaches are given in Sec. II. After discussion of the first-chance emission process (Sec. III), this model will be generalized for multiple particle emission (MPE) in Sec. IV. Finally, it will be applied to calculations of neutron and proton (double-differential) emission cross sections. The results which cover quite a large range of nuclear masses ($A \geq 27$) and incident energies (5-26 MeV) are presented in Sec V.

II. SMD-SMC MODEL

A. Basic formalism

The differential cross section for a reaction (a, b) is given by

$$\frac{d\sigma_{ab}(E_a)}{dE_b} = \frac{4\pi^3}{k_a^2} |T_{ab}|^2 \delta(E_a - E_b), \quad (1)$$

where the T matrix can be written as

$$T_{ab} = \sum_{nv} c_{nv}^{b*} \langle \varphi_{nv}^{(-)} | T | \varphi_a^{(+)} \rangle. \quad (2)$$

Here, the final wave function is decomposed into states of exciton classes $n = p + h$ (of the composite system A), ν is a running index in class n . In the many-body theory,¹⁹ the transition operator T is expanded in powers of the irreducible effective interaction \hat{I} ,

$$T = \hat{I} + \hat{I}G_0T. \quad (3)$$

The irreducible interaction $\hat{I}_{n,n'}$ is a sum of different Feynman graphs (containing the bare NN interaction) which cannot be cut into parts by just cutting n lines. The Green's function (GF) in Eq. (3) is a product of n single-particle (s.p.) GF's. It has the spectral representation

$$G_0(n, n) = \sum_{\nu} \frac{\varphi_{n\nu} \varphi_{n\nu}^*}{E - e_{n\nu}} + \sum_{\nu c} \frac{\varphi_{n\nu c}^{(+)} \varphi_{n\nu c}^{(+)*}}{E - E_{n\nu c} + i\eta} \\ = G_B(n, n) + G_U(n, n), \quad (4)$$

where $\varphi_{n\nu}$, $\varphi_{n\nu c}^{(+)}$ are bound and bound eigenfunctions of $H_0 + \hat{I}_{n,n}$ with eigenvalues $e_{n\nu}$ and $E_{n\nu c} = e_{n-1,\nu} + E_c + B_c$, respectively. Here, $E_c = \hbar k_c^2 / 2m$ and B_c are the kinetic and binding energies of the unbound nucleon.

It is especially convenient if both the bound and unbound GF's in Eq. (4) are split into one pole part and one smoothly energy-dependent regular part. Then we may convert¹⁹ Eq. (3) to an expression which contains the pole parts of G_0 only,

$$T = I + I(G_U^{(+)} + G_B^{(+)})T, \quad (5)$$

while the regular parts of G_0 are used for a renormalization of the effective interaction,

$$I = \hat{I} + \hat{I}(G_U^R + G_B^R)I. \quad (6)$$

This effective interaction in the form of (mean) squared matrix elements enters the further treatment as a main ingredient. According to the splitting in Eq. (4) we have to distinguish between four types of elements, I_B , I_{BU} , I_{UB} , and I_U denoting the coupling between bound and/or unbound states.

In nuclear physics it becomes customary to decompose Eq. (5) into two parts,

$$T = T^U + T^U G_B^{(+)} T \equiv T^U + T^B, \quad (7)$$

where the multistep direct part is given by the Born series,

$$T^U = I + I G_U^{(+)} T^U, \quad (8)$$

and the multistep compound part has the form

$$T^B = T^U G_B^{(+)} T^U + T^U G_B^{(+)} T^U G_B^{(+)} T^U + \dots \quad (9a)$$

Similar (approximative) expressions were derived either within a shell-model approach¹ or projection operator formalism.² However, the approximation $T^U \equiv I$ by some authors^{2,3} was used in Eq. (9a). Following Ref. 1 we extend this approximation by an additional term, $I G_U^{(+)} I$, which yields the matrix element

$$T_{ab}^B = I_{UB} (G_B^{(+)} - I_B - I_{BU} G_U^{(+)} I_{UB})^{-1} I_{BU}. \quad (9b)$$

In contrast to the multistep direct processes, Eq. (8), the multistep compound series in Eqs. (9) describes processes in which the nuclear system undergoes at least one transition to stages in which all particles occupy bound orbitals characterized by $G_B^{(+)}$. Thus, a single-step contribution occurs only in Eq. (8).

B. Statistical assumptions

For complex nuclei and sufficient high incident energies, the cross section in Eq. (1) cannot be evaluated microscopically. Analytical expressions are obtained for energy-averaged cross sections only. This fact is also governed by the finite energy resolution of the experimental facilities. The energy uncertainty of the incident beam leads to an average over quasibound levels of the composite system A , while the finite detector resolution causes an exit-channel averaging (i.e., it averages over the eigenstates in the residual nucleus, $A - 1$).

It is well known¹⁰ that incident-energy averages taken over levels of the A -body system yield the decomposition

$$T_{ab}(E_a) = \langle T_{ab}(E_a) \rangle_A + T_{ab}^{fl}(E_a) \quad (10)$$

with $\langle T_{ab}^{fl} \rangle_A = 0$.

Since Eq. (8) is assumed to depend smoothly on incident energy, we have

$$\langle T_{ab}(E_a) \rangle_A \simeq T_{ab}(E_a + i\Delta_a) \simeq T_{ab}^U(E_a), \quad (11)$$

where the averaging width is taken as $\Delta_a \simeq 0.1 - 1.0$ MeV. Comparing Eqs. (7) and (10), it yields $T_{ab}^{fl} \simeq T_{ab}^B$, and via Eq. (1), also

$$\left\langle \frac{d\sigma_{ab}}{dE_b} \right\rangle_A = \frac{4\pi^3}{k_a^2} (|T_{ab}^U|^2 + \langle |T_{ab}^B|^2 \rangle_A) \delta(E_a - E_b). \quad (12)$$

Now, if we take an exit-channel average (denoted by angular brackets carrying the subscript $A - 1$) we arrive at analytical expressions for both the SMD and SMC cross sections,

$$\left\langle \left\langle \frac{d\sigma_{ab}}{dE_b} \right\rangle_A \right\rangle_{A-1} = \frac{d\sigma_{ab}^{\text{SMD}}}{dE_b} + \frac{d\sigma_{ab}^{\text{SMC}}}{dE_b}. \quad (13)$$

The statistical assumptions are defined by treating the effective interaction as a random matrix taken from Gaussian orthogonal ensembles (GOE).^{1,6,10} Then, the first moments of all elements (mean value) vanish and the second moments are defined by

$$\overline{I_{n\nu n'\nu'} I_{m\mu m'\mu'}} = (\delta_{nm} \delta_{\nu\mu} \delta_{n'm'} \delta_{\nu'\mu'} + \delta_{nm'} \delta_{\nu\mu} \delta_{n'm} \delta_{\nu'\mu'}) \overline{I_B^2}(n, n'). \quad (14a)$$

Equation (14a) is defined for the bound-bound case. Similarly we have for other cases (in a more compact prescription)

$$\overline{I_{UB} I_{UB}^*} = \overline{I_{UB}^2}(nc, n'), \quad \overline{I_{BU} I_{BU}^*} = \overline{I_{BU}^2}(n, n'c'), \quad (14b)$$

$$\overline{I_U I_U^*} = \overline{I_U^2}(nc, n'c'). \quad (14c)$$

Here the upper contraction lines denote an averaging over the A -body ensemble while the bottom lines indicate $(A - 1)$ -body ensemble averaging. In addition, both ensembles are assumed to be statistically uncorrelated.

The channel index $c = \{E_c, \Omega_c, \nu, \text{ or } \pi\}$ will be chosen as kinetic energy, direction, and particle type (neutron or proton) of the unbound particle. Further, $E = E_a + B_a$ and $U = E - B_b - E_b$ are the excitation energies of the composite and residual systems.

TABLE I. Energy and deformation parameter of two low-lying phonon states of multipolarity 2^+ and 3^- .

Target	ω_2 (MeV)	β_2	ω_3 (MeV)	β_3
²⁷ Al, ²⁸ Si	1.78	0.41	6.88	0.22
⁴⁸ Ti	0.98	0.27	3.00	0.14
⁵¹ V	1.55	0.17	3.00	0.14
⁵² Cr	1.43	0.22	4.59	0.18
⁵⁵ Mn	0.83	0.25	4.60	0.18
⁵⁶ Fe	0.85	0.24	4.52	0.18
⁵⁸ Ni	1.45	0.18	4.47	0.18
⁵⁹ Co	1.33	0.21	4.05	0.17
⁶⁵ Cu	1.35	0.18	3.70	0.16
⁹¹ Zr	2.19	0.09	2.25	0.13
⁹³ Nb	0.93	0.13	2.30	0.18
⁹⁴ Zr	0.92	0.09	2.12	0.12
⁹⁴ Mo	0.87	0.15	2.53	0.13
⁹⁶ Mo	0.78	0.17	2.24	0.13
⁹⁸ Mo	0.79	0.17	2.50	0.13
¹⁰⁰ Mo	0.54	0.23	1.91	0.12
¹⁰⁷ Ag	0.51	0.23	2.07	0.12
¹¹² Cd, ¹¹³ Cd	0.35	0.22	1.97	0.12
¹¹⁵ In	1.29	0.11	1.95	0.12
¹¹⁸ Sn	1.30	0.11	2.32	0.13
¹²¹ Sb	1.17	0.11	2.39	0.13
¹²⁷ I	0.44	0.18	2.30	0.13
¹²⁸ Te	0.74	0.14	2.50	0.13
¹⁸¹ Ta	0.09	0.07	1.50	0.10
¹⁸⁶ W	0.12	0.08	1.50	0.10
²⁰⁸ Pb, ²⁰⁹ Bi	4.08	0.05	2.62	0.14

C. Restricted partial state densities

The partial (or exciton) state density of the composite system results from the pole part of the bound GF (after averaging)

$$\begin{aligned} \frac{i}{\pi} G_B^{(+)}(n, n) &\rightarrow \sum_{\nu} \delta(E - e_{n\nu}) = \sum_{\{j_k\}} \delta \left[E - \sum_{k=1}^{p+h} e_{j_k} \right] \\ &= \frac{g(gE)^{n-1}}{p!h!(n-1)!} \\ &\equiv \rho_n(E) \end{aligned} \quad (15)$$

and is given in the independent-particle model (IPM) by the Ericson formula.²⁰ Here, the density of the mean-

field single-particle and hole states j_k of energy e_{j_k} are approximated by g , i.e., the s.p. state density at Fermi energy $\varepsilon_F \approx 40$ MeV. By the same token, the exciton state density $\rho_{n-1}(U)$ of the residual system is obtained from $G_U^{(+)}$. All these results are derived from the assumption that the effective interaction changes the exciton number without any restriction.

The formulas alter drastically if k -body forces are assumed which change the exciton number by $\Delta n = n_f - n_i = -k, -k+2, \dots, k-2, k$. As a consequence, $\rho_n(E)$ and $\rho_{n-1}(U)$ tend to the restricted partial state densities $\rho_n^{(\Delta n)}(E)$ and $\rho_n^{(\Delta n-1)}(U)$, respectively. They are defined by

$$\rho_n^{(\Delta n-i)}(\mathcal{E}) = \rho_n^{-1}(E) \sum_{p_i} \sum_{\{j_k\}} \delta \left[E - \sum_{k=1}^n e_{j_k} \right] \int_0^{\mathcal{E}} dt \delta \left[t - \sum_{k=1}^{n-n_i} e_{j_k} \right] \delta \left[\mathcal{E} - t - \sum_{k=1}^{n_f-i} e_{j_k} \right], \quad (16)$$

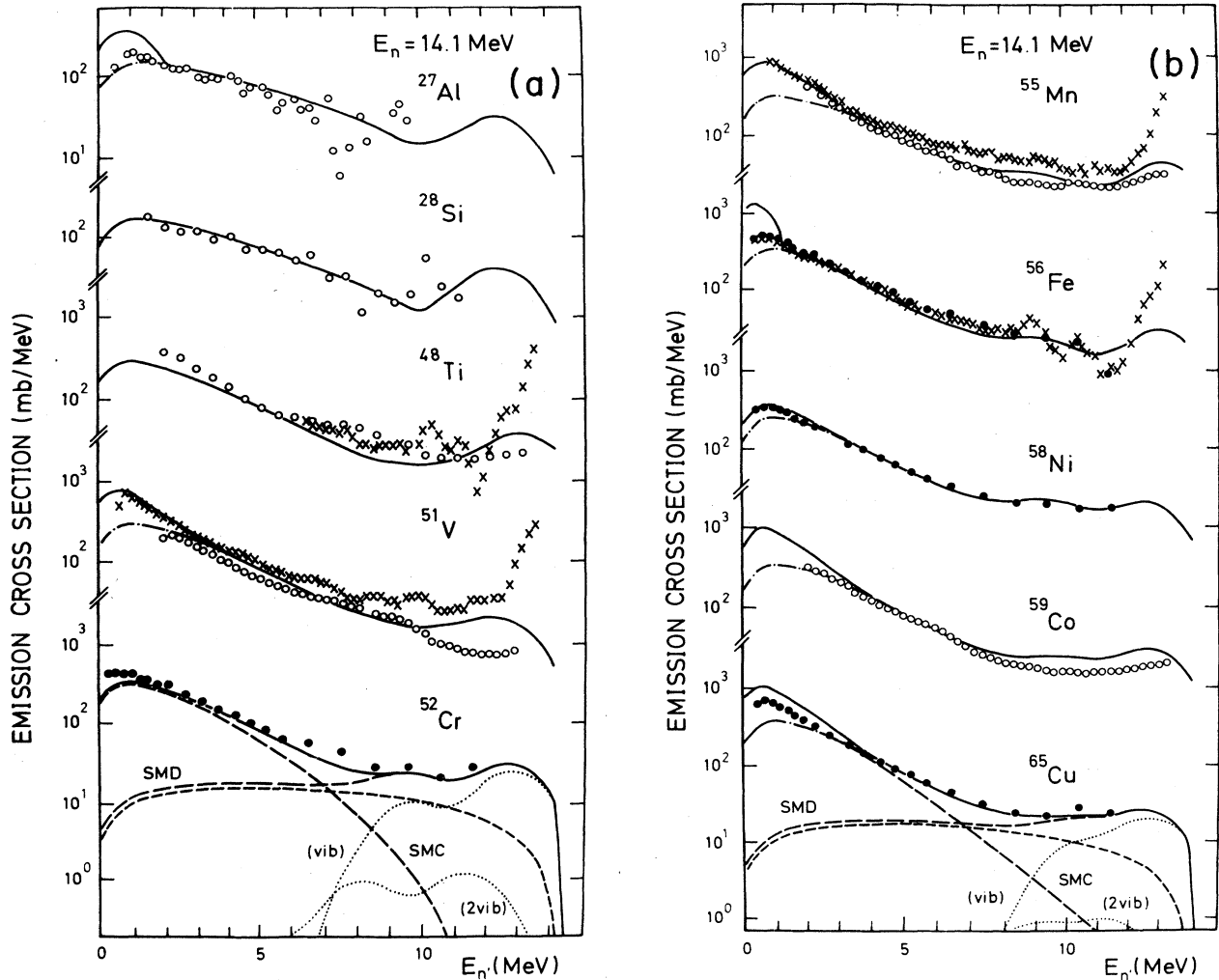


FIG. 1. (a) Angle-integrated (n, xn) spectra for various nuclei at 14-MeV incident energy. Experimental data from Ref. 38 (open circles), Ref. 39 (closed circles), and Ref. 40 (crosses). For denotations see the text. (b) Same as (a). (c) Same as (a) but crosses denote experimental data from Ref. 30. (d) Same as (a) but crosses denote experimental data from Ref. 30. (e) Same as (a) but crosses denote experimental data from Ref. 30.

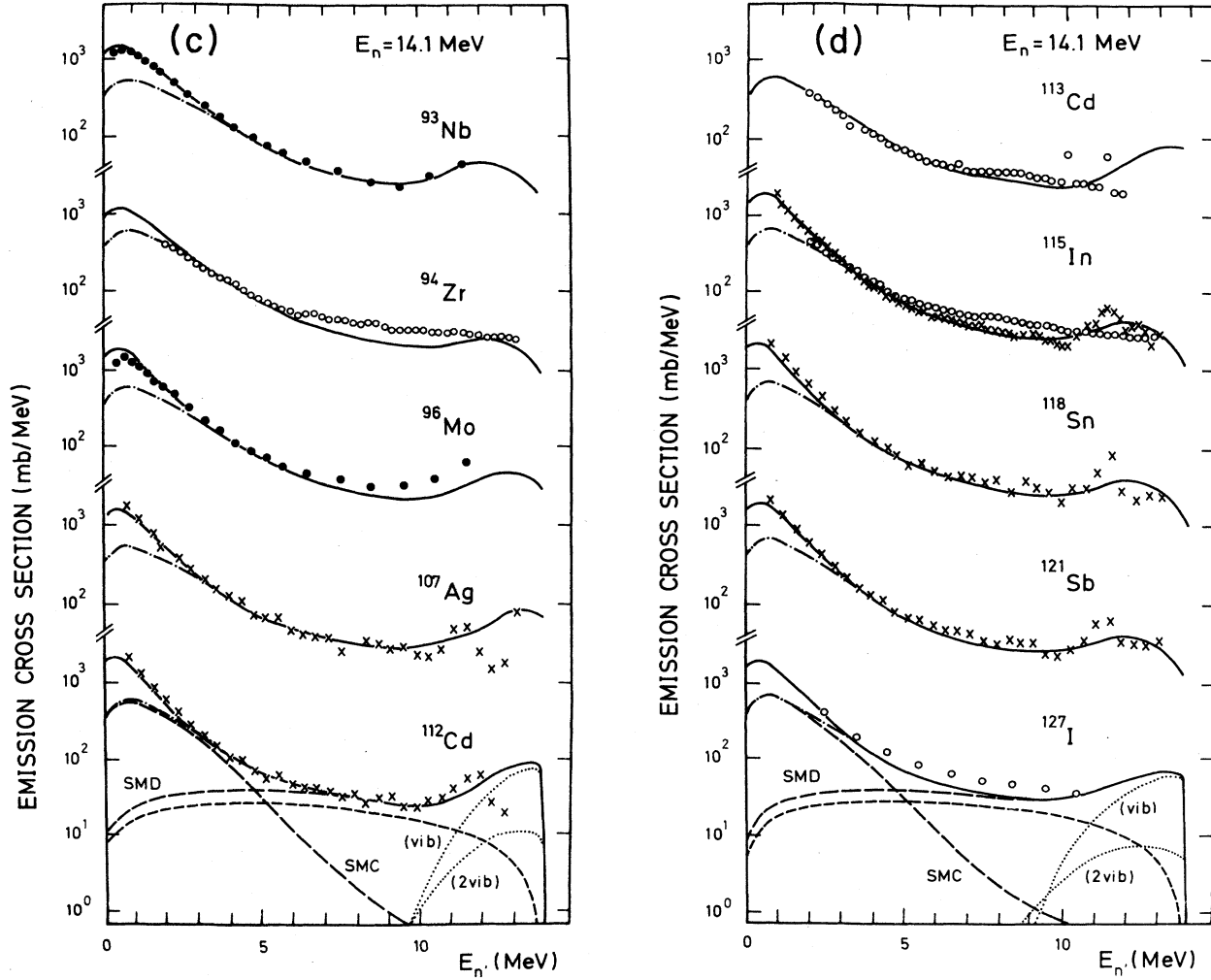


FIG. 1. (Continued).

where $n_i = p_i + h_i$ and $n_f = p_f + h_f$ denote the numbers of active particles and holes before and after the collision. Mathematically, the k -body assumption is connected with a transition from GOE to the embedded GOE (EGOE).¹⁸ Comparing Eqs. (15) and (16) the GOE and EGOE quantities are related by

$$\rho_n(E) = \sum_{(\Delta n)} \rho_n^{(\Delta n)}(E), \quad (17)$$

where the sum runs in two steps over all values $\Delta n \leq |n|$.

Starting out from Eq. (16) and assuming two-body forces, we obtain the (two-body) restricted partial state densities of both the composite system, $\rho_n^{(\Delta n)}(E)$, and the residual system, $\rho_n^{(\Delta n-1)}(U)$. The former enter the damping widths $\Gamma_n^{(\Delta n)} \downarrow$ and were first suggested by Williams²¹ (cf. also Ref. 22). The latter, which enter the escape widths $\Gamma_{nb}^{(\Delta n)}(E_b) \uparrow$, were first pointed out in Ref. 2.

D. Residual interaction

The explicit values of all mean-squared matrix elements defined in Eqs. (14) are obtained in three steps: (i)

The dependence on the exciton number is absorbed into the (two-body) restricted partial state densities introduced above. (ii) All types of unbound mean-squared matrix elements are reduced to bound-bound ones, $\bar{I}_B^2 = (V_0/A)^2$, where V_0 is the strength of the residual interaction,

$$V(\mathbf{r}_1, \mathbf{r}_2) = -V_0 \frac{4}{3} \pi r_0^3 \delta(\mathbf{r}_1 - \mathbf{r}_2).$$

(iii) Finally V_0 is found by equating the optical model (OM) reaction cross section to the same quantity evaluated from the particle-hole concept.

The reduction to \bar{I}_B^2 is realized (approximately) by

$$\bar{I}_{BU}^2(E_b) = \bar{I}_B^2(2s+1)\rho(E_b) \equiv \bar{I}_B^2 \rho^{(\text{out})}(E_b), \quad (18a)$$

(cf. Ref. 23), as well as

$$\bar{I}_{UB}^2(E_a) = \rho^{(\text{in})}(E_a) \bar{I}_B^2, \quad (18b)$$

$$\bar{I}_U^2(E_a, E_b) = \rho^{(\text{in})}(E_a) \bar{I}_B^2 \rho^{(\text{out})}(E_b), \quad (18c)$$

where

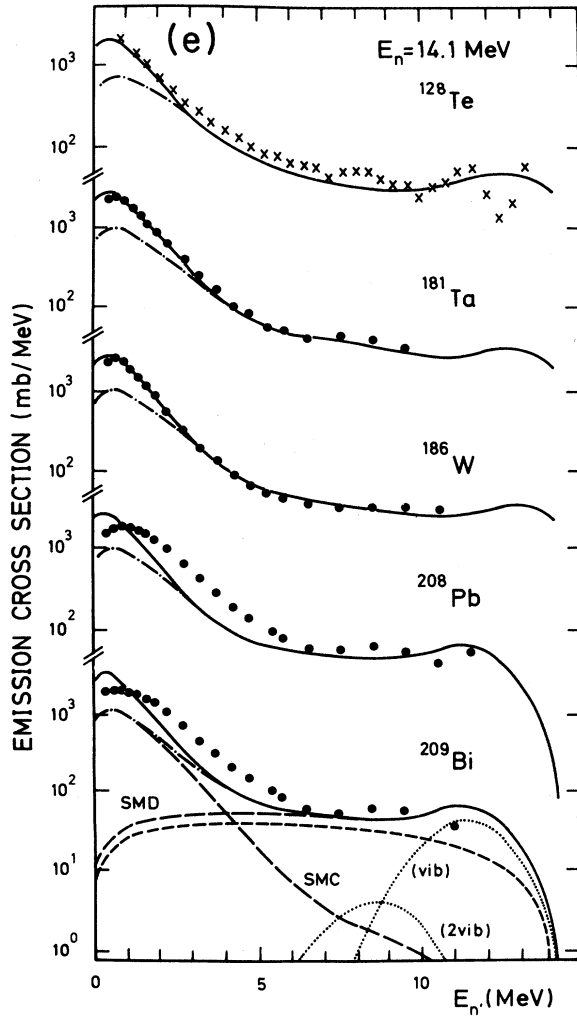


FIG. 1. (Continued).

$$\rho^{(in)}(E_c) = (2s+1)^{-1} (k_c R)^{-2} \rho(E_c). \quad (19a)$$

Here,

$$\rho(E_c) = \frac{2}{3} \sum_l (2l+1) \frac{R}{\pi} \frac{1}{\hbar v_c} = \frac{4\pi \mathcal{V} m k_c}{(2\pi)^3 \hbar^2} \quad (20)$$

is the sp state density in the nuclear volume, $\mathcal{V} = 4\pi R^3/3$, and $R = r_0 A^{1/3}$. The value of the radius parameter $r_0 = 1.40$ fm was obtained from the relation (in MeV^{-1})

$$2(2s+1)\rho(\epsilon_F) \equiv g = A/13, \quad (21)$$

where the factor 2 contains the isospin degeneracy.

If a surface-delta interaction is assumed

$$V(\mathbf{r}_1 - \mathbf{r}_2) = -V_0 \frac{4\pi}{3} r_0^4 \delta(\mathbf{r}_1 - \mathbf{r}_2) \delta(\mathbf{r}_1 - \mathbf{R}), \quad (22)$$

then Eq. (19a) changes into

$$\rho_{\text{surf}}^{(in)}(E_c) = (r_0/R)^2 \rho^{(in)}(E_c). \quad (19b)$$

Even this parametrization, rather than Eq. (19a), pro-

vides a correct A dependence of the OM reaction cross section (for neutrons and $E_a \geq 5$ MeV)

$$\sigma_v^{\text{OM}}(E_a) = (4\pi^3/k_a^2) \overline{I_{\text{UB}}^2}(E_a) \rho_1^{(\Delta n=2)}(E), \quad (23)$$

which is the formation cross section of a $2p1h$ -doorway state starting out from a $1p$ configuration. Using

$$\begin{aligned} \rho_1^{(\Delta n=2)}(E) &= (g_N^2 + g_Z^2) \int_0^E dE_c (E - E_c) (2s+1) \rho(E_c + \epsilon_F + B_c) \\ & \quad (24) \end{aligned}$$

and $g_N = (N/A)g$, $g_Z = g - g_N$, the value $V_0 \approx 19.4$ MeV was obtained from Eq. (23). [This value, together with Eq. (19b), coincides with the parametrization given in Ref. 17.] It will be used for all SMD calculations.

Coulomb effects, i.e., the dependence of unbound mean-squared matrix elements on particle types ν and π are treated in a simple way: Equation (20) should be multiplied by the penetration factor, $\mathcal{P}_c(E_c)$, defined in Ref. 15.

E. SMC processes

According to Eq. (13) the SMC cross section is obtained^{16,17} from Eq. (9b) using the contraction technique¹ as

$$\begin{aligned} \frac{d\sigma_{ab}^{\text{SMC}}(E_a)}{dE_b} &= \frac{4\pi^3}{k_a^2} \langle \langle T_{ab}^B T_{ab}^{B*} \delta(E_a - E_b) \rangle \rangle_{A-1} \\ &= \sigma_a^{\text{SMC}}(E_a) \sum_n \frac{\tau_n}{\hbar} [\Gamma_{nb}^{(0)}(E_b) \uparrow + \Gamma_{nb}^{(-)}(E_b) \uparrow], \end{aligned} \quad (25)$$

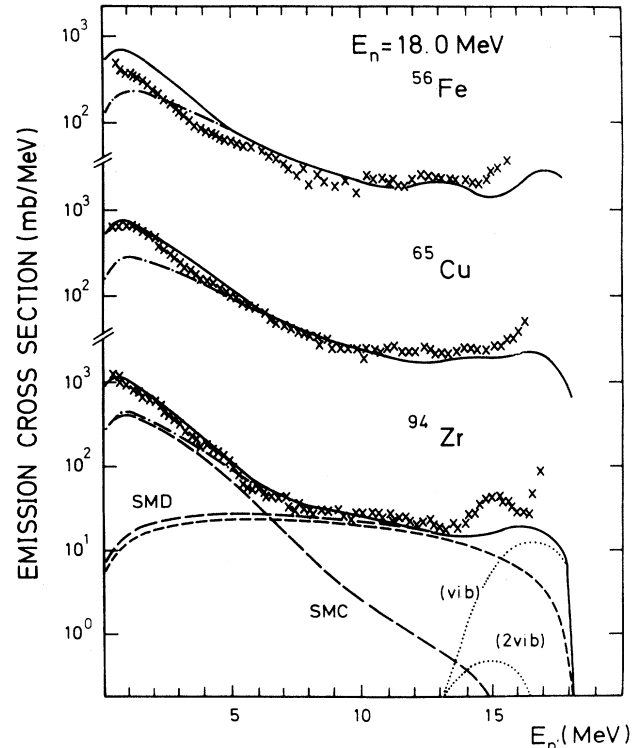


FIG. 2. Same as Fig. 1(a) but at 18-MeV incident energy.

where τ_n satisfies the time-integrated master equation,

$$-\hbar\delta_{nn_0} = \Gamma_{n-2}^{(+)}\downarrow\tau_{n-2} + \Gamma_{n+2}^{(-)}\downarrow\tau_{n+2} - \Gamma_n\tau_n. \quad (26)$$

The superscripts (+), (0), and (-) refer to $\Delta n = +2, 0, -2$, respectively. Here, the damping and escape widths are given by

$$\Gamma_n^{(\Delta n)\downarrow} = 2\pi I_B^2 \bar{\rho}_n^{(\Delta n)}(E), \quad (27)$$

$$\Gamma_{nb}^{(\Delta n)}(E_b)\uparrow = 2\pi I_{BU}^2 \bar{\rho}_n^{(\Delta n-1)}(U), \quad (28a)$$

$$\Gamma_n^{(\Delta n)\uparrow} = \sum_{b=\nu,\pi} \int_0^{E-E_b} dE_b \Gamma_{nb}^{(\Delta n)}(E_b)\uparrow. \quad (28b)$$

The total width is

$$\Gamma_n = \Gamma_n^{(+)\downarrow} + \Gamma_n^{(-)\downarrow} + \Gamma_n^{(0)\uparrow} + \Gamma_n^{(-)\uparrow}.$$

Notice that an escape mode $\Gamma_n^{(+)\uparrow}$ is absent since it is impossible from energetical arguments. The sum over the exciton number in Eq. (25) runs from $n_0=3$ up to

$(2gE)^{1/2}$ which includes the equilibrium stage $\bar{n} \simeq (1.4gE)^{1/2}$.

It is an advantage of the parametrization in Eq. (18a) that all I_B^2 cancel exactly within the sum of Eq. (25). Thus, the shape of the SMC emission spectra becomes independent of I_B^2 .

Finally, the normalization constant in Eq. (25) is approximated by

$$\sigma_a^{\text{SMC}}(E_a) \equiv \sum_b \sigma_{ab}^{\text{SMC}}(E_a) = \sigma_a^{\text{OM}}(E_a) - \sum_b \sigma_{ab}^{\text{SMD}}(E_a), \quad (29)$$

which is dictated by flux conservation. Here, σ_{ab}^{SMD} signifies the (energy-integrated) SMD cross section given below.

F. SMC versus the exciton model

For the sake of completeness we have to mention in which sense the SMC model, Eq. (25), differs from the

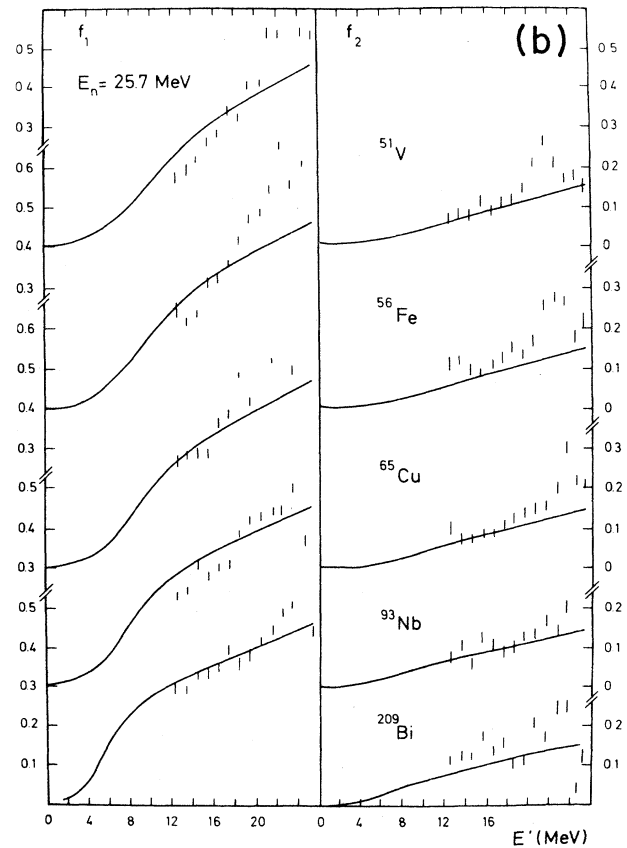
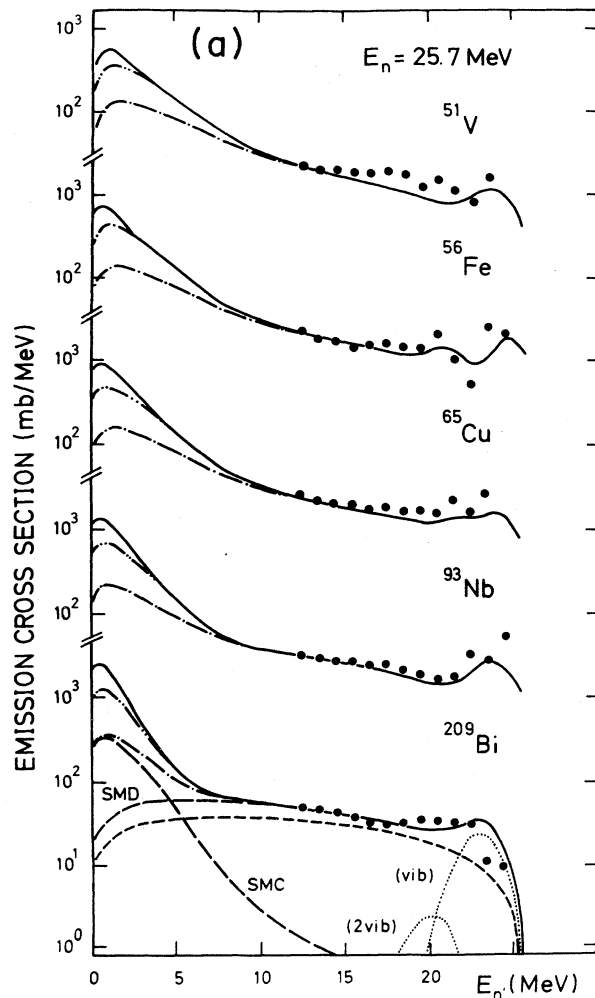


FIG. 3. (a) Same as Fig. 1(a) but at 25.7-MeV incident energy. Experimental data from Ref. 41. (b) Legendre coefficients f_1 and f_2 of (n, xn) spectra depicted in (a).

phenomenological exciton model^{24,25} (EM),

$$\frac{d\sigma_{ab}^{\text{EM}}(E_a)}{dE_b} = \sigma_a^{\text{OM}}(E_a) \sum_n \frac{\tau_n}{\hbar} \Gamma_{nb}^{\text{EM}}(E_b) \uparrow. \quad (30)$$

Within the EM the escape widths

$$\Gamma_{nb}^{\text{EM}}(E_b) \uparrow = \frac{(2s+1)}{\pi^2 \hbar^2} m E_b \sigma_n^{\text{inv}}(E_b) \frac{p(n-1)}{gE} \left(\frac{U}{E} \right)^{n-2}, \quad (31)$$

are obtained from a detailed balance principle. Therein the inverse cross section is approximated by the OM reaction cross section,

$$\sigma_n^{\text{inv}}(E_b) \simeq \sigma_b^{\text{OM}}(E_b). \quad (32)$$

However, this is not always true since the exciton number dependence is ignored. More precisely, the inverse cross section should be defined as

$$\sigma_n^{\text{inv}}(E_b) = (4\pi^3/k_b^2) \overline{I_{\text{BU}}^2}(E_b) \rho_n^{(0)}(E) \quad (33)$$

rather than Eq. (32). After inserting Eq. (33) into Eq. (31)

the relation¹⁶

$$\Gamma_{nb}^{\text{EM}}(E_b) \uparrow \simeq \Gamma_{nb}^{(0)}(E_b) \uparrow \quad (34)$$

is found. Hence, the EM follows immediately from the SMC model if (i) the backward escape mode is neglected, $\Gamma_{nb}^{(-)}(E_b) \uparrow \equiv 0$, and (ii) direct reactions are absent, $\sigma_{ab}^{\text{SMD}} \equiv 0$, which yield, in Eq. (29), $\sigma_a^{\text{SMC}} = \sigma_a^{\text{OM}}$.

It is clear from the above that the approximation in Eq. (32) prohibits a cancellation of $\overline{I_B^2}$ within the EM. Thus $\overline{I_B^2}$ is treated as a fit parameter in the EM.

G. SMD processes

The SMD cross section follows from Eq. (8) as

$$\begin{aligned} \frac{d\sigma_{ab}^{\text{SMD}}(E_a)}{dE_b} &= \frac{4\pi^3}{k_a^2} \langle T_{ab}^U T_{ab}^{U*} \delta(E_a - E_b) \rangle_{A-1} \\ &= \sum_{r=1} \frac{d\sigma_{ab}^{(r)}(E_a)}{dE_b}. \end{aligned} \quad (35)$$

Before evaluating Eq. (35) we have to distinguish¹⁰ be-

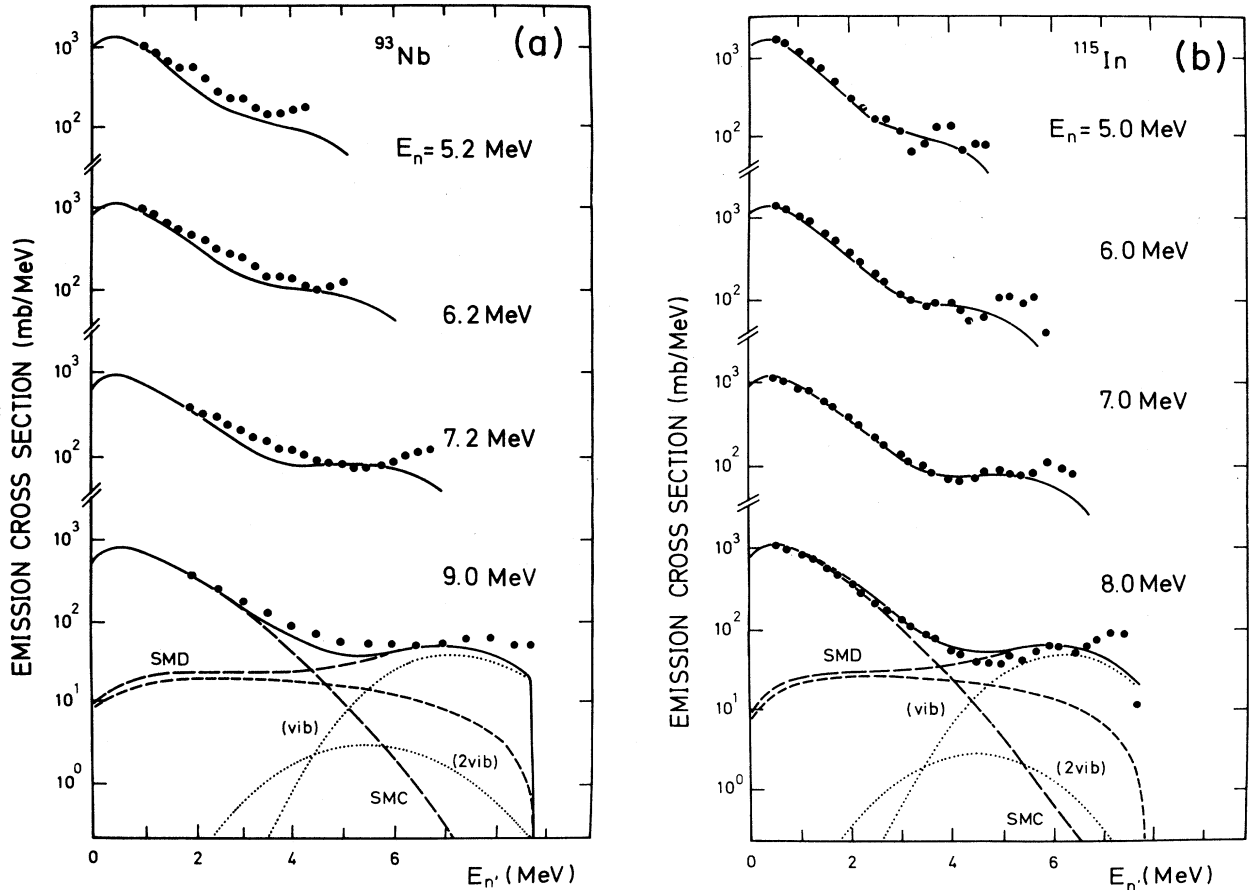


FIG. 4. (a) Angle-integrated (n,xn) spectra for ^{93}Nb at different incident energies. Experimental data from Refs. 29 and 42 (at $E_n = 9$ MeV). For denotations see the text. (b) Same as (a) but for ^{115}In . Experimental data from Ref. 43.

tween the sudden and adiabatic approximations. However, within the independent-particle model (IPM), and using the parametrization in Eqs. (19), both approximations coincide.¹⁷ Thus, for the one-step and two-step processes we have (despite a kinematical factor $4\pi^3/k_a^2$)

$$\frac{d\sigma_{ab}^{(1)}(E_a)}{dE_b} = \overline{I_U^2}(E_a, E_b) \rho_1^{(+)}(E_a - E_b), \quad (36a)$$

$$\begin{aligned} \frac{d\sigma_{ab}^{(2)}(E_a)}{dE_b} &= \int \frac{dE_1}{4\pi} \overline{I_U^2}(E_a, E_1) \\ &\times 2\pi^2 \rho_1^{(+)}(E_a - E_1) \overline{I_U^2}(E_1, E_b) \\ &\times \rho_1^{(+)}(E_1 - E_b) \end{aligned} \quad (36b)$$

with the restricted partial state densities $\rho_1^{(+)}(U) = (g_N^2 + g_Z^2)U$.

To include collective modes (of multipolarity λ , energy ω_λ , and deformation parameter β_λ) we decompose¹⁵⁻¹⁷ the transition probability,

$$I_{U\rho_1}^{2(+)}(U) \longrightarrow \overline{I_U^2} \rho_1^{(+)}(U) + \sum_{\lambda} \overline{I_{\lambda}^2} \delta(U - \omega_{\lambda}). \quad (37)$$

The ansatz for the particle-vibration coupling

$$I_{\lambda}^2 = \hat{\beta}_{\lambda}^2 V_R^2 (k_a R)^{-2} \rho(E_a) \rho(E_b) \quad (38)$$

can be obtained after replacing in Eq. (22) the quantity

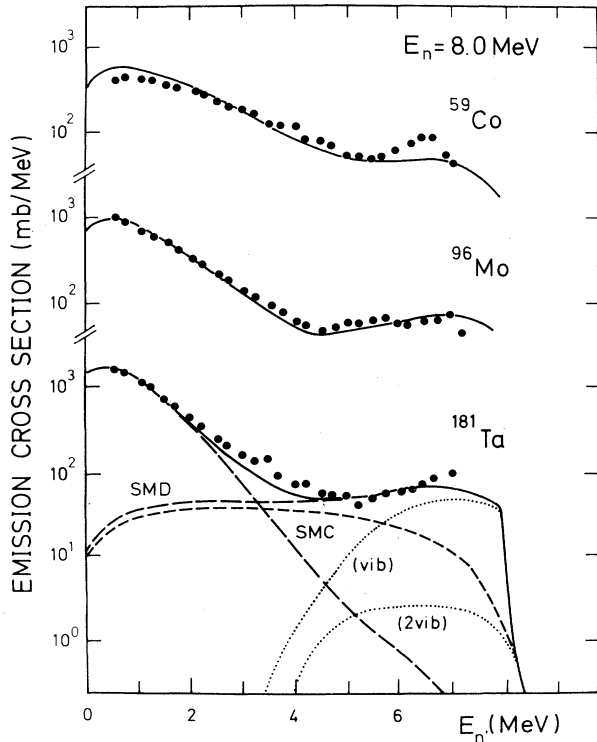


FIG. 5. Angle-integrated (n,xn) spectra for ^{59}Co , ^{96}Mo , and ^{181}Ta at 8-MeV incident energy. Experimental data from Ref. 43. For denotations see the text.

$V_0 r_0 \delta(r-R)$ by $\hat{\beta}_{\lambda} V_R R \delta(r-R)$, where

$$\hat{\beta}_{\lambda} \equiv [4\pi(2\lambda+1)]^{-1/2} \beta_{\lambda}.$$

Here, $V_R \simeq 48$ MeV is the real potential depth.

Starting out from Eqs. (36), (37), and (19b) we finally obtain simple expressions for the SMD cross section,

$$\frac{d\sigma_{ab}^{[\alpha]}(E_a)}{dE_b} = \left[\frac{m\gamma}{2\pi\hbar^2} \right]^2 \frac{4\pi}{(k_a R)^2} [\alpha] \frac{k_b}{k_a} \mathcal{P}_a(E_a) \mathcal{P}_b(E_b), \quad (39)$$

where $[\alpha]$ symbolizes two one-step and four two-step contributions, denoted according to the sequence of excitation and phonon excitations,

$$\alpha_{\text{ex}} = \mathcal{R}_{ab} (V_0 A^{-4/3} g)^2 U, \quad (40a)$$

$$\alpha_{\text{vib}} = \delta_{ab} \sum_{\lambda} \hat{\beta}_{\lambda}^2 V_R^2 \delta(U - \omega_{\lambda}), \quad (40b)$$

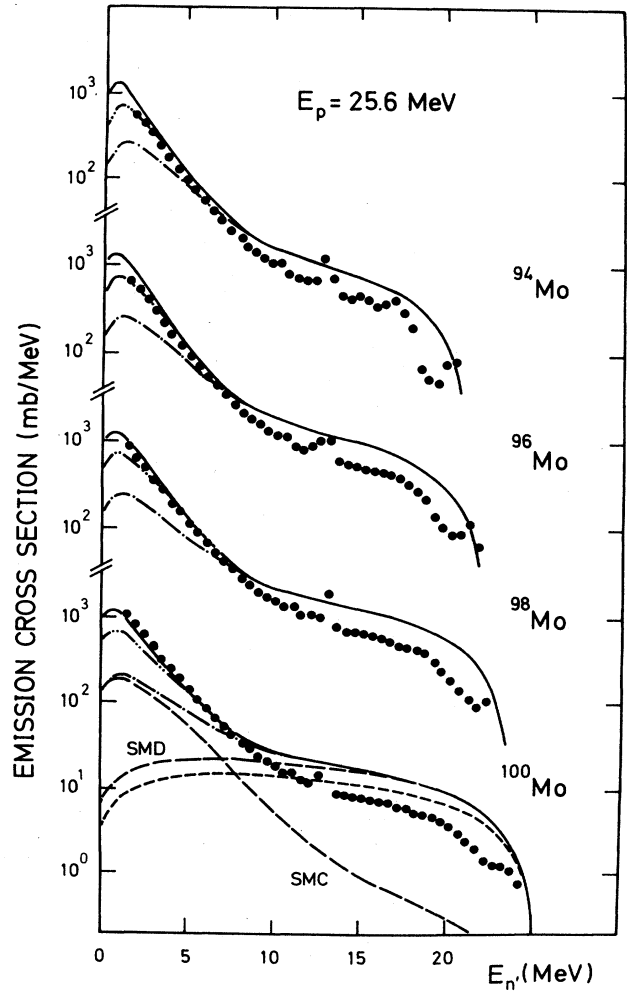


FIG. 6. Angle-integrated (p,xn) spectra for $^{94,96,98,100}\text{Mo}$ at 25.6-MeV incident energy. Experimental data from Ref. 44. For denotations see the text.

$$\alpha_{2\text{ex}} = \mathcal{R}_{ab} \mathcal{R}_{bb} (V_0 A^{-4/3} g)^4 q_1 U^3 / 6, \quad (41a)$$

$$\alpha_{\text{ex,vib}} = \alpha_{\text{vib,ex}} = \mathcal{R}_{ab} (V_0 A^{-4/3} g)^2 q_1 \sum_{\lambda} \hat{\beta}_{\lambda}^2 V_r^2 (U - \omega_{\lambda}), \quad (41b)$$

$$\alpha_{2\text{vib}} = \delta_{ab} \sum_{\lambda, \lambda'} \hat{\beta}_{\lambda}^2 \hat{\beta}_{\lambda'}^2 V_R^4 q_1 \delta(U - \omega_{\lambda} - \omega_{\lambda'}). \quad (41c)$$

The combinatorial factor is given by

$$A^2 \mathcal{R}_{ab} = \delta_{ab} (N^2 + Z^2) + (1 - \delta_{ab}) (N^2 \delta_{b\nu} + Z^2 \delta_{b\pi}) \quad (42)$$

and

$$q_1 = \frac{1}{2} \pi (k_1 R)^{-2} \rho^2(E_1).$$

III. FIRST-CHANCE EMISSION

The first-chance emission will be evaluated within the SMD-SMC model as

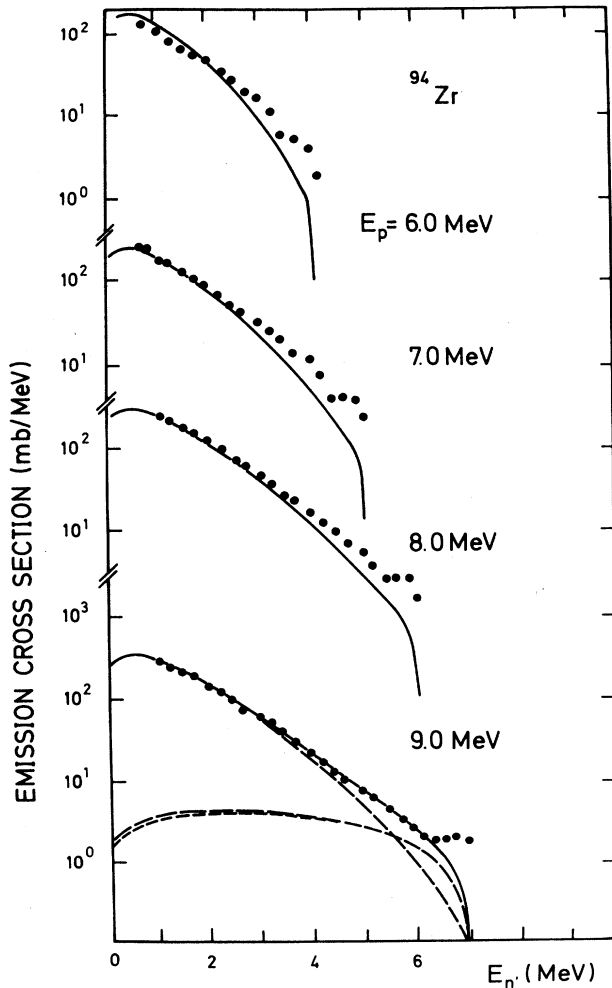


FIG. 7. Same as Fig. 6 but for ^{94}Zr at different incident energies. Experimental data from Ref. 45.

$$\frac{d^2 \sigma_{a,b}(E_a)}{dE_b d\Omega_b} = \frac{d\sigma_{ab}^{\text{SMD}}(E_a)}{dE_b} \sum_{L=0} \frac{2L+1}{4\pi} a_L(E_b) P_L(\cos\theta) + \frac{1}{4\pi} \frac{d\sigma_{ab}^{\text{SMC}}(E_a)}{dE_b}. \quad (43)$$

Here, the angular distribution of SMC emission is assumed to be isotropic, while for the SMD processes the empirical systematics of Kalbach and Mann²⁶ are adopted.

Since the SMD process terminates after a few collisions, we restrict ourselves to one-step and two-step contributions for the incident energy range below 30 MeV. All SMD calculations are performed with the residual interaction strength $V_0 = 19.4$ MeV. In case of phonon excitations, we restrict ourselves to two low-lying vibrational states of multipolarity $\lambda^\pi = 2^+$ and 3^- . For odd-mass nuclei the weak-coupling model²⁷ was adopted. The phonon parameters β_2 and ω_2 are taken from Ref. 28 (except for ^{93}Nb where Ref. 29 was used). Otherwise, ω_3 are received from Refs. 27, 30, and 31. All β_3 parameters are calculated from

$$\beta_{\lambda}^2 = (2\lambda + 1) \omega_{\lambda} / 2C_{\lambda} \quad (44)$$

with $C_3 = 500$ MeV. In summary, all parameters used in the calculations are listed in Table I. Moreover, the delta functions entering Eqs. (40b) and (41c) are replaced by Gaussians of width 1 MeV simulating both the limited (exit-channel) energy resolution in the experiments and the spreading of spectroscopic strength.

The SMC processes are calculated by adopting the restricted partial state densities of Refs. 2 and 21. Both Pauli and pairing corrections are considered by an energy shift,³²

$$a_{ph}^A = A_{ph} \{ 1 + [2g\Delta(A)/n]^2 \}^{1/2} + \frac{g}{4} [\Delta_0^2(A) - \Delta^2(A)], \quad (45)$$

where $A_{ph} = (p^2 + h^2 + p - 3h)/4g$. The ground-state correlation function $\Delta_0(A) = \Delta_0(N, Z)$ depends on the neutron and proton numbers in the nuclear systems. This quantity can be obtained from the condensation energy $C(N, Z) = g\Delta_0^2/4$ inferred from odd-even (*o/e*) mass differences. More explicitly, $C(e, e) = \Delta_N + \Delta_Z - \delta$, $C(e, o) = \Delta_N$, $C(o, e) = \Delta_Z$, and $C(o, o) = 0$ where Δ_N , Δ_Z , and δ are taken from the systematics in Ref. 33. Thereafter, the excited-state correlation function $\Delta(n, U)$ will be calculated analytically³² from Δ_0 .

The energy shift defined in Eq. (45) enters the restricted partial state densities in different modifications. More precisely, we have

$$\rho_n^{(+)}(E) = \frac{g^3 (E - a_{p+1, h+1}^A)^2}{2(n+1)} \left[\frac{E - a_{p+1, h+1}^A}{E^*} \right]^{n-1}, \quad (46a)$$

$$\rho_n^{(-)}(E) = \frac{gph(n-2)}{2} \left[\frac{E - a_{p-1, h-1}^A}{E^*} \right]^{n-1}, \quad (46b)$$

which enter the damping widths in Eq. (27) and $E^* = E - a_{ph}^A$. Similarly, the residual excitation energy U which enters $\rho_n^{(\Delta n-1)}(U)$ in the escape widths should be replaced by

$$U = E - B_b - E_b - a_{p+\Delta p, h+\Delta h}^{A-b}, \quad (47)$$

whereas the energy denominator, E , in Eqs. (5.16)–(5.18) of Ref. 2 should be changed into E^* . In Eq. (47) the abbreviations $\Delta p = \Delta n/2 - 1$ and $\Delta h = \Delta n/2$ hold.

IV. EMISSION SPECTRA

A. General considerations

The double-differential cross section (DDX) for the reaction (a,xb) is given by

$$\frac{d^2\sigma_{a,xb}(E_a)}{dE_b d\Omega_b} = \frac{d\sigma_{a,xb}(E_a)}{dE_b} \times \sum_{L=0}^{\infty} \frac{2L+1}{4\pi} f_L^{(a,xb)}(E_a, E_b) P_L(\cos\theta), \quad (48)$$

where the differential cross section (energy spectrum),

$$\frac{d\sigma_{a,xb}(E_a)}{dE_b} = \frac{d\sigma_{a,b}}{dE_b} + \sum_c \frac{d\sigma_{a,cb}}{dE_b} + \sum_{c,d} \frac{d\sigma_{a,cdb}}{dE_b} + \dots, \quad (49)$$

is a sum of first-chance emission, second-chance emission, etc. Assuming isotropic multiple particle emission, the Legendre coefficients in Eq. (48) simplify to ($L \geq 1$)

$$f_L^{(a,xb)}(E_a, E_b) = \left[\frac{d\sigma_{ab}^{\text{SMD}}(E_a)}{dE_b} / \frac{d\sigma_{a,xb}(E_a)}{dE_b} \right] a_L(E_b). \quad (50)$$

Henceforth, the particle-type indices $a, b = n, p$, and γ denote neutron, proton (it should not be confused with exciton and particle number introduced above), and γ ray.

The following (model-independent) relations for energy-integrated cross sections should be satisfied (at incident energy E_a)

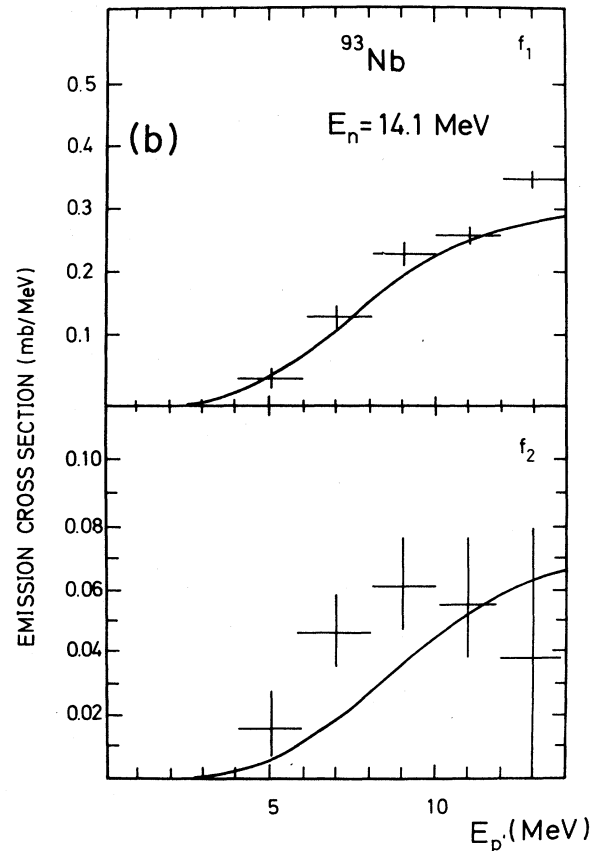
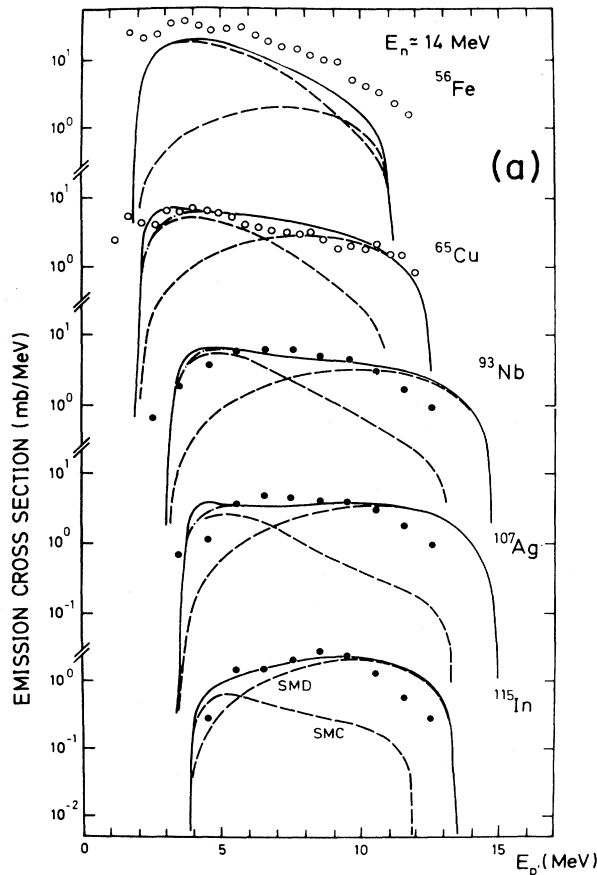


FIG. 8. (a) Angle-integrated (n, xp) spectra for different nuclei at 14-MeV incident energy. Experimental data from Ref. 46 (^{56}Fe , ^{65}Cu), Ref. 47 (^{93}Nb), and Ref. 48 (^{107}Ag , ^{115}In). For denotations see the text. (b) Legendre coefficients f_1 and f_2 of (n, xp) spectrum for ^{93}Nb at 14-MeV incident energy.

$$\sigma_{a,xb} = \sigma_{a,b} + \sum_c \sigma_{a,cb} + \sum_{c,d} \sigma_{a,cdb} + \dots, \quad (51)$$

where the partial cross sections are given by

$$\sigma_{a,b} = \sum_c \sigma_{a,bc} \quad (52a)$$

and

$$\sigma_{a,bc} = \sum_d \sigma_{a,bcd},$$

etc. In this context the OM reaction cross section is defined as

$$\sigma_a^{\text{OM}}(E_a) = \sum_b \sigma_{a,b}(E_a). \quad (52b)$$

Now, adopting Eqs. (52), the total emission cross section in Eq. (51) can be cast into a form which contains excitation functions (e.g., measured by activation technique) only,

$$\begin{aligned} \sigma_{a,xb} = & \sigma_{a,b\gamma} + \sum_c (\sigma_{a,bc\gamma} + \sigma_{a,cb\gamma}) \\ & + \sum_{c,d} (\sigma_{a,bcd\gamma} + \sigma_{a,cbd\gamma} + \sigma_{a,cdb\gamma}) + \dots, \end{aligned} \quad (53)$$

where $b, c, d \neq \gamma$. Neglecting charged-particle emission, Eq. (53) reduces to

$$\sigma_{a,xn} = \sum_{v=1} \nu \sigma_{a,vn}. \quad (54)$$

Otherwise, for example, the $(a, 2n\gamma)$ -excitation function can be calculated by the relation

$$\sigma_{a,2n\gamma} = \sigma_{a,2n} - \sigma_{a,3n}. \quad (55)$$

B. Multiple particle emission

The MPE is treated as a pure SMC approach. Hence, Eq. (25) will be used, but it should be modified in two respects.

(i) The residual excitation energy U given in Eq. (47) which enters the escape widths should be replaced by

$$U = E - B_c - B_{cb} - E_b - a_p^{A-c-b} \frac{1}{p+\Delta p, h+\Delta h} \quad (56a)$$

for the second-chance emission (a, cb) , and by

$$U = E - B_c - B_{cd} - B_{cdb} - E_b - a_p^{A-c-d-b} \frac{1}{p+\Delta p, h+\Delta p} \quad (56b)$$

for the third-chance emission (a, cdb) , respectively. The quantities B_{cb} and B_{cdb} are the binding energies of particle b in the residual systems $(A-c)$ and $(A-c-d)$.

(ii) The normalization constant in Eq. (25) should be replaced by $(\sigma_{a,c} - \sigma_{a,c\gamma})$ for the (a, cb) process and by $(\sigma_{a,cd} - \sigma_{a,cd\gamma})$ for the (a, cdb) process, respectively. Approximative expressions for the γ -emission processes are

$$\sigma_{a,c\gamma}(E_a) = \int_{E-B_c-B_{c\nu}}^{E-B_c} dE_c [d\sigma_{a,c}(E_a)/dE_c], \quad (57a)$$

$$\begin{aligned} \sigma_{a,cd\gamma}(E_a) & \\ & = \int_{E-B_c-B_{cd}-B_{cd\nu}}^{E-B_c-B_{cd}} dE_d [d\sigma_{a,cd}(E_a)/dE_d]. \end{aligned} \quad (57b)$$

All other SMC quantities entering Eqs. (25) and (26) remain the same as in the first-chance emission case, i.e., the damping widths given by Eqs. (27) and (46) as well as the energy denominator within the escape widths are both referred to $E^* = E - a_{ph}^A$. Since the escape widths for MPE via Eqs. (56) become much smaller compared to the first-chance emission the mean lifetimes τ_n in the master equation (26) increase rapidly. Notice that here τ_n is the mean lifetime of exciton class n in the composite system A with reference to the emission of more than one particle.

In comparison with other MPE approaches,³⁴ in our simple formalism the master equation has to be solved one time only for each MPE process ($\sigma_{a,cb}$, $\sigma_{a,cdb}$, etc.). Formally, this model looks very similar to a simple cascade-evaporation procedure where an average emission-energy shift (caused by the previous emitted particle) in Eqs. (56) is roughly simulated by the Pauli and pairing corrections a_{ph}^A .

V. RESULTS

To prove the consistency of the predicted SMD-SMC model, neutron, and proton spectra (n, xn) and (n, xp) , as well as (p, xn) including three decays of the compound system, are calculated by code EXIFON (Ref. 35) for about 30 nuclei between $A=27$ and 209 at incident energies between 5 and 25 MeV. Using throughout the same parameters [$g=A/13$, $r_0=1.40$ fm, $V_R=48$ MeV, and $V_0=19.4$ MeV, which is the surface-delta interaction strength in Eq. (22)] a *global description* was performed. Further, all binding energies are taken from Ref. 36. The OM reaction cross sections are calculated analytically³⁷ (Wilmore-Hodgson for neutrons, Bechetti-Greenlees for protons). All phonon parameters are listed in Table I (cf. Sec. III). The running time on a personal computer (IBM AT) is 5–50 s per nucleus depending on incident energy.

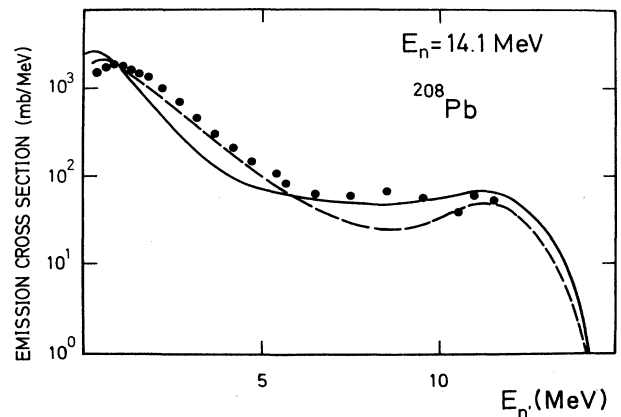


FIG. 9. Angle-integrated (n, xn) spectra for ^{208}Pb at 14.1 MeV for $g = A/13$ (solid line) and $g = A/26$ (dashed line).

The results are depicted and compared with experimental data^{29,30,38-48} in Figs. 1-9. (The meaning of the curves is the same in all figures. Dot-dashed line: first-chance emission; dot-dot-dashed line: first-chance plus second-chance emission; long-dashed line: SMD or SMC separately; short-dashed line: α_{ex} contribution; dotted lines: α_{vib} and α_{2vib} contributions separately; solid line: total emission spectrum.) We see that despite the great simplicity of the model it is successful in reproducing experimental emission spectra for both different incident energies and different nuclei. This holds for energy as well as angular distributions. The latter are shown for neutron [Fig. 3(b)] and proton emissions [Fig. 8(b)] in the form of the first two Legendre coefficients.

In summary, the following conclusions can be drawn.

(i) Ignoring shell effects, a fair description of emission spectra was obtained by adopting global parameters only. However, special care is required for magic nuclei where the sp state density g strongly deviates from the global value $A/13$. This is the main reason for the discrepancy in the description of ²⁰⁸Pb and ²⁰⁹Bi at 14 MeV in Fig. 1(e). The influence of the emission spectrum on g is demonstrated in Fig. 9 where calculations for ²⁰⁸Pb with $g = A/13$ and $A/26$ are compared.

(ii) Whereas for the SMC description no nuclear structure information is used (e.g., cancellation of I_B^2), the calculation of SMD processes, e.g., the excitation of collective modes, requires spectroscopic values ($\beta_\lambda, \omega_\lambda$).

(iii) Whereas the proposed MPE model predicts the right spectral shape for the second- and third-chance emission (cf. Fig. 6), the magnitude of MPE calculation in the threshold energy region overestimates the experimental data. Here, the magnitude of MPE as well as the SMC cross section is determined only by a normalization constant in Eq. (25). For MPE the latter is too high since

in Eqs. (57) so far a correct γ competition is absent. Also (n, α) processes are ignored. Thus, especially for light and medium nuclei (²⁷Al, ⁵⁶Fe, ⁵⁹Co, and ⁶⁵Cu in Figs. 1 and 2), discrepancies in the low emission-energy region occur.

(iv) As shown in Figs. 6 and 8(a) for (p, n) and (n, p) reactions, the calculated one-step direct contribution which influences the high-energy tail of the spectra overestimates the experiments. It results from Eq. (40a) which is a rather crude approximation for charge-exchange processes.

To this end we continue with some general remarks of how a (n, n') process is composed of the following.

(i) The ratio of SMD to SMC contributions increases with incident energy and is close to 1 at 30-MeV incident energy.

(ii) The one-step contribution dominates. It is about 18% (30%) of the OM reaction cross section at 14 (26) MeV incident energy. Otherwise, for the two-step contributions, we have 3% (10%) at 14 (26) MeV. The ratios are independent of mass number.

(iii) While the integral contribution of direct particle-hole excitations rises with incident energy ($\alpha_{ex} \sim A^{2/3} E_a$ and $\alpha_{2ex} \sim A^{4/3} E_a^3$) it decreases for phonon excitations. At about 10 MeV we have $\alpha_{ex} \approx \alpha_{vib}$.

(iv) The ratio of two-phonon to one-phonon excitations is almost independent of A and E_a . It takes the value $\alpha_{2vib}/\alpha_{vib} \approx 0.1$.

(v) Direct three-step processes, α_{3vib} , are very small and thus can be neglected for incident energies below 26 MeV.

The authors are grateful to Lien Hoang Ngoc from National Atomic Energy Institute Hanoi for support in performing the calculations.

¹D. Agassi, H. A. Weidenmüller, and G. Mantzouranis, Phys. Rep. **22**, 145 (1975).

²H. Feshbach, A. Kerman, and S. E. Koonin, Ann. Phys. (N.Y.) **125**, 429 (1980).

³F. A. Zhivopistsev and V. G. Sukharevsky, Phys. Elem. Particle Nuclei, Dubna **15**, 1208 (1984).

⁴Sadhan K. Adhikari, Phys. Rev. C **31**, 1220 (1985).

⁵K. W. McVoy and X. T. Tang, Phys. Rep. **94**, 139 (1983).

⁶H. Nishioka, J. J. M. Verbaarschot, H. A. Weidenmüller, and S. Yoshida, Ann. Phys. (N.Y.) **172**, 67 (1986).

⁷P. Mädlar and R. Reif, Nucl. Phys. A **373**, 27 (1982).

⁸T. Tamura, T. Udawaga, and H. Lenske, Phys. Rev. C **26**, 379 (1982).

⁹R. Reif, Acta Phys. Slovaca **25**, 208 (1975).

¹⁰H. Nishioka, H. A. Weidenmüller, and S. Yoshida [submitted to Ann. Phys. (N.Y.)].

¹¹M. Herman, A. Marcinkowski, and K. Stankiewicz, Nucl. Phys. A **430**, 69 (1984).

¹²G. M. Field, R. Bonetti, and P. E. Hodgson, J. Phys. G **12**, 93 (1985).

¹³Gargi Keeni, Z. Phys. A **325**, 327 (1986).

¹⁴R. Bonetti, M. Camnasio, L. Colli-Milazzo, and P. E. Hodgson, Phys. Rev. C **24**, 71 (1981).

¹⁵H. Kalka, D. Seeliger, and F. A. Zhivopistsev, Z. Phys. A **329**, 331 (1988).

¹⁶H. Kalka, Proceedings of the 17th International Symposium on Nuclear Physics, Gaussig, 1987, edited by H. Kalka and D. Seeliger (Zentralinstitut für Kernforschung Report ZfK-646, 1988, pp. 24-38); in Proceedings of the Workshop on Applied Nuclear Theory and Nuclear Model Calculations for Nuclear Technology, Trieste, 1988 (unpublished).

¹⁷H. Kalka and D. Seeliger, Proceedings of the 5th International Symposium on Nuclear Induced Relations, Smolenice, 1988 (unpublished).

¹⁸T. A. Brody, J. Flores, J. B. French, P. A. Mello, A. Pandey, and S. M. Wong, Rev. Mod. Phys. **53**, 385 (1981).

¹⁹A. B. Migdal, *Theory of Finite Fermi Systems and Applications to Nuclei* (Wiley Interscience, New York, 1970).

²⁰T. Ericson, Adv. Phys. **9**, 425 (1960).

²¹F. C. Williams, Phys. Lett. **31B**, 181 (1970).

²²P. Obložinsky, I. Ribansky, and E. Betak, Nucl. Phys. A **266**, 347 (1974).

- ²³E. V. Lee and J. J. Griffin, *Phys. Rev. C* **5**, 1713 (1972).
- ²⁴M. Blann, *Annu. Rev. Nucl. Sci.* **25**, 123 (1975).
- ²⁵K. Seidel, D. Seeliger, R. Reif, and V. D. Toneev, *Phys. Elem. Particle Nuclei, Dubna* **7**, 499 (1976).
- ²⁶C. Kalbach and F. M. Mann, *Phys. Rev. C* **23**, 112 (1981).
- ²⁷A. Bohr and B. R. Mottelson, *Nuclear Structure* (Benjamin, Reading, 1975), Vol. 2.
- ²⁸S. Raman, C. H. Malarkey, W. T. Milner, C. W. Nestor, and P. H. Stelson, *At. Data Nucl. Data Tables* **36**, 1 (1987).
- ²⁹S. P. Simakov, G. N. Lovchikova, V. P. Lunev, O. A. Salnikov, and N. N. Titarenko, *Yad. Fiz.* **37**, 801 (1983).
- ³⁰Y. Watanabe, I. Kumabe, M. Hyakutake, A. Takahashi, H. Sugimoto, E. Ichimura, and Y. Sasaki, *Phys. Rev. C* **37**, 163 (1988).
- ³¹E. Fretwurst, G. Lindström, K. F. von Reden, V. Riech, S. I. Vasiljev, P. P. Zarubin, O. M. Knyazkov, and I. N. Kuchtina, *Nucl. Phys.* **A468**, 247 (1987).
- ³²C. Y. Fu, *Nucl. Sci. Eng.* **86**, 344 (1984).
- ³³D. G. Madland and J. R. Nix, *Nucl. Phys.* **A476**, 138 (1988).
- ³⁴J. M. Akkermans and H. Gruppelaar, *Z. Phys. A* **300**, 345 (1981).
- ³⁵H. Kalka, code EXIFON version, 1988 (unpublished).
- ³⁶Y. Ando, M. Uno, and M. Yamada, Japan Atomic Energy Research Institute Report JAERI-M 83-025, 1983.
- ³⁷A. Chatterjee, K. H. N. Murthy, and S. K. Gupta, *Pramana* **16**, 391 (1981).
- ³⁸D. Hermsdorf, A. Meister, S. Sassonoff, D. Seeliger, K. Seidel, and F. Shahin, Zentralinstitut für Kernforschung Report ZfK-277, 1974.
- ³⁹A. Pavlik and H. Vonach, IRK report, 1988.
- ⁴⁰M. Baba, M. Ishikawa, N. Yabuta, T. Kikuchi, H. Wakabayashi, and N. Hirakawa, Proceedings of the International Conference on Nuclear Data for Science and Technology, Mito, 1988 (unpublished).
- ⁴¹A. Marcinkowski, R. W. Finlay, G. Randers-Pehrson, C. E. Brient, R. Kurup, S. Mellema, S. Meigooni, and R. Tailor, *Nucl. Sci. Eng.* **93**, 13 (1983).
- ⁴²M. Adel-Fawzy, H. Förtsch, S. Mittag, D. Schmidt, D. Seeliger, and T. Streil, EXFOR 32001, IAEA-NDS (1982).
- ⁴³S. P. Simakov, G. N. Lovchikova, O. A. Salnikov, and N. N. Titarenko, *Yad. Fiz.* **38**, 3 (1983).
- ⁴⁴E. Mordhorst, M. Trabandt, A. Kaminsky, H. Krause, W. Scobel, R. Bonetti, and F. Crepsi, *Phys. Rev. C* **34**, 103 (1986).
- ⁴⁵G. N. Lovchikova (private communication).
- ⁴⁶M. Grimes, R. C. Haight, K. R. Alvar, H. H. Barschall, and R. R. Borchers, *Phys. Rev. C* **19**, 2127 (1979).
- ⁴⁷G. Traxler, A. Chalupka, R. Fischer, B. Strohmaier, M. Uhl, and H. Vonach, *Nucl. Sci. Eng.* **90**, 174 (1985).
- ⁴⁸R. Fischer, M. Uhl, and H. Vonach, *Phys. Rev. C* **37**, 578 (1988).